BURST PRESSURE ASSESSMENT OF CORRODED PIPELINES SUBJECTED TO PERMANENT GROUND DEFORMATION

B.C. Mondal[1*], R. J. Suki[2] and T. J. Khan[3]

[1]Professor, Department of Civil Engineering, CUET, Bangladesh, email: bipul@cuet.ac.bd
[2]Department of Civil Engineering, CUET, Bangladesh, email: u1701045@student.cuet.ac.bd
[3]Department of Civil Engineering, CUET, Bangladesh, email: u1701078@student.cuet.ac.bd

***Corresponding Author**

ABSTRACT

Steel pipelines are used extensively in the oil and gas industries due to their high strength to weight ratio. The structural integrity of pipelines in areas prone to landslides poses a significant challenge due to the combined effects of corrosion and permanent ground deformation (PGD). In this study, the effects of PGD on the behaviour of corroded pipelines were investigated numerically. The corroded pipelines of an X80 high-grade steel were modelled using Finite Element Method (FEM). Through a series of Finite Element Analyses considering different corrosion geometries, and varying levels of PGD, the remaining strength of the pipelines, in terms of internal pressure, were determined. This investigation resulted in the construction of failure envelopes those account for different corrosion parameters and intensities of PGD. The failure envelope will provide valuable insights for the design, construction, and maintenance of pipelines located in hilly or landslide-prone terrains.

Keywords: *Landslide, PGD, Corrosion, Finite Element Method, Failure envelope*

1. INTRODUCTION

Metals naturally corrode when exposed to the environment, causing entropy and energy release. Corrosion weakens pipes, leading to uneven pressure distribution, especially in defective areas. The fluid carried by the pipe exerts pressure internally in all directions and corrosion defects resist the internal pressure from distributing uniformly at the defective zone, but the pressure concentrates at that area. The metal of the pipe undergoes a thinning process, which causes adverse effects on properties like yield strength and ultimate tensile strength. The phenomenon gets worse when the pipeline system faces severe permanent ground deformation after a major seismic hazard, movement of the fault line, landslides due to heavy rain, or debris flow withdrawing material. High stresses develop at the defective area due to imposed deformation, shear, and bending loads and may cause failure of the pipeline (Vazouras et al. 2010). The potentiality of a pipeline being shifted by a lateral or vertical movement of soil depends on pipe steel properties, soil-pipe interaction, the behaviour of materials, the depth of buried pipe, the amount, and the expeditiousness of the ground movement (Lee et al. 2016). The structural integrity of the buried pipeline across a hazardous area is endangered consistently, even at a small ground deformation. Understanding corroded pipeline failures during landslides is vital for safe operation and maintenance. An in-depth assessment of these pipelines is necessary.

The mechanical behaviour of a buried pipeline under a strike slip fault was investigated with FE analysis and it was concluded that a soft ground results in a large deformation and stiff ground results in relatively less deformation (Vazouras et al. 2010). A parametric solution for active loading of soil upon buried pipelines was generated considering the magnitudes of active loading and resistance acting on the pipeline and estimated the maximum deflection and stresses by Randolph et al. (2010). However, they imposed limitations due to some simplified assumptions. A two-dimensional finite element model was developed by Zhu and Randolph (2010) considering plain strain conditions and restraining the pipe with a set of springs to evaluate the impact of landslide on the pipeline.

Regarding the mechanical response of gas pipelines during landslides, various studies have contributed valuable insights. Using LS-DYNA software and a specialised model, research was conducted to investigate the mechanical behaviour of underground steel pipelines across landslide areas (Liao et al. 2021). Strain demands on buried steel pipelines were analysed with a three dimensional (3-D) nonlinear beam-Winkler spring FE analysis. The steel pipelines were subjected to different ground deformation patterns considering both longitudinal and lateral movement with different magnitudes (Agbo et al. 2022). The mechanical response of pipelines under lateral landslides, utilising methods such as the R-O model and a simplified approach, were examined (Rajani et al. 1995 and Rourke et al. 1995).

Short term effect of PGD and corrosion defect was combined to analyse the failure probability by changing the value of bending moment and with the progress of corrosion defect (Benjamin et al. 2007). Multiple corrosion growth directions were used instead of a simplified conservative corrosion model (Wang et al. 2020).

Finite element analysis was performed to characterise the mechanical behaviour of buried pipelines crossing landslide areas, considering soil-pipe interaction (Zhang et al. 2016). Zang et al. (2020) and Cao et al. (2020) utilised the finite element method to investigate how landslides affect buried pipelines within landslide-prone sections. These studies collectively contribute to understanding the intricate relationship between landslide disasters and pipeline integrity. There is a need for more research on the consequences of both landslide catastrophes and pipeline corrosion on the remaining strength (i.e., burst pressure) of pipelines.

Existing researches focus on corrosion dimensions like defect depth and length to analyse the failure pressure of defected pipelines but in the case of a landslide loading on a defected pipe, failure pressure analysis is in lack of investigation. For a safe operation, the remaining strength determination should go under a vigorous investigation. In this study, a failure envelope is constructed using the 3-D FE

analysis to predict the burst pressure of corroded pipelines subjected to permanent ground deformation (PGD).

2. FINITE ELEMENT MODEL

Numerical analysis is a useful tool to conduct a parametric study. Three-dimensional (3-D) continuum FE analysis was performed using Abaqus software in this study. The parts for soil and pipeline were developed using brick element (Abaqus element name, C3D8R). The geometrical and mechanical properties of the pipeline are given in Table 1. The dimensions of the soil domain are shown in Figure 1. Figure 1 (a) shows the dimensions of the soil profile along the longitudinal direction of the pipeline and Figure 1 (b) shows the 3-D view of the soil domain. The dimensions are collected from Gu et al. (2022). The top surface of the soil domain is inclined by 30° in the transverse direction.

Table 1: Properties of pipe (Gu et al. 2022)

Diameter	Length	Wall thickness	Density	Poisson's ratio	Modulus of elasticity
1016 mm	80 m	22 mm	7800 kg.m^{-3}	0.3	20600 MPa

There are two compositions in the soil body, one is the sliding part, and the other is the non-sliding part. The sliding portion is 20 m wide and located at the central part of the soil body. The rest of the soil portions are 30 metres on both sidesof the sliding portion. The pipeline is placed perpendicular to the direction of soil movement below 2 m of the soil top. In general, transverse and longitudinal ground movements are two different directions of ground movement in relation to the pipeline's axial direction. According to existing literature, the probability of soil movement is higher along the transverse direction compared to the longitudinal direction (Wang et al. 2020). Therefore, the pipeline is placed perpendicular to the soil movement direction.

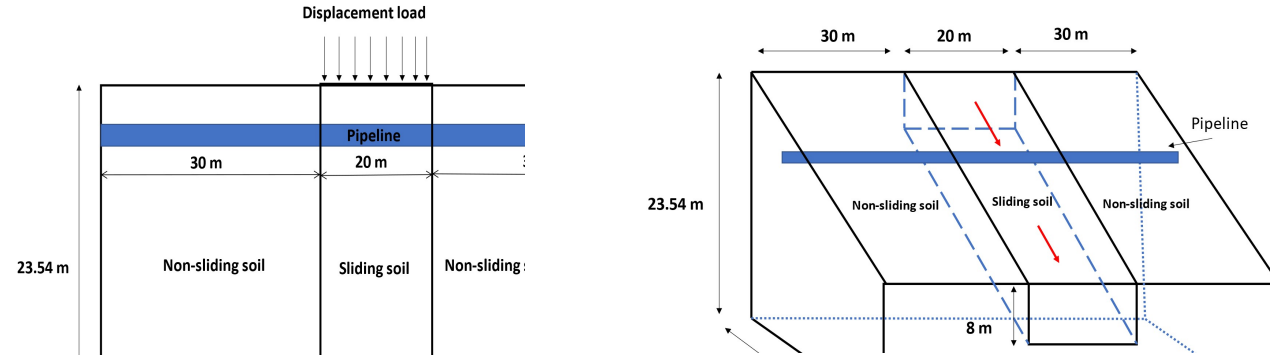

(a) Soil Profile along longitudinal direction (b) 3-D view of Soil Domain

Figure 1: Dimensions of Soil Domain (After Gu et al. 2022)

2.1 Material Models

Nowadays, the pipelines are made of high-grade steel. A pipe made of X80 grade steel is considered in this study. The non-linear stress–strain relationships of X80 grade steel is shown in Figure 2 (Gu et al. 2022). Other properties of X80 grade steel are given in Table 1.

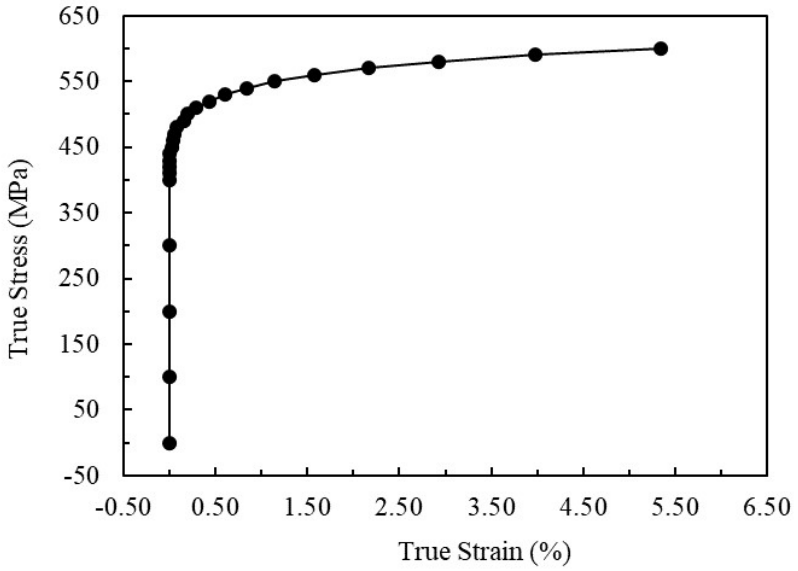

Figure 2: True Stress–True Strain Curve of X80 Grade Steel (After Gu et al. 2022)

For the soil body, different soil properties, given in Table 2, are applied to two different parts, i.e., sliding part and non-sliding part (shown in Figure 1).

Table 2: Properties of soil (Gu et al. 2022)

Parameter:	Density ($kg \cdot m^{-3}$)	Poisson's ratio	Elastic modulus (MPa)	Internal friction (°)	Cohesion (Kpa)	Friction coefficient
Sliding Soil:	1900	0.4	20	20	20	0.4
Sliding Soil:	2040	0.35	32.5	-	-	-

To simulate pipe–soil interaction, hard contact penalty function is used for the tangential behaviour of the soil which represents a firm estimation of hard contact. From the existing literature, it is worth noticing that an impact on the result is found with a friction coefficient between 0.2 to 0.4 (Vazouras et al. 2010). The friction coefficient of 0.4 is used in this study. Hard contact Pressure-Overclosure is maintained in this case and separation is allowed after contact.

2.2 Meshing and Boundary Conditions

Using the advantages of symmetricity, the half model is developed in this study to save the computation time. Symmetric boundary conditions are applied at the symmetric surface and the other end of the model is fully restrained. Similarly, the bottom surface of the soil body is fully restrained. To simulate permanent ground displacement (PGD) of the sliding soil part, a transverse displacement load inclined by 30° with the base of the soil body is applied at the rear face of the sliding soil part as shown in Figure 1.

During meshing the model, fine mesh is applied at the top part of the soil domain where the soil movement is expected, whereas the coarse mesh is applied at the remaining part of the soil domain. The pipe domain is meshed with the mesh size similar to the soil mesh size attached to the pipes' outer surface. Four layers of elements are provided through the wall thickness of the pipeline following the recommendation of British Standard (BS 7910 2013). Mesh sensitivity analysis is performed to obtain the optimum mesh size. A typical mesh size is shown in Figure 3.

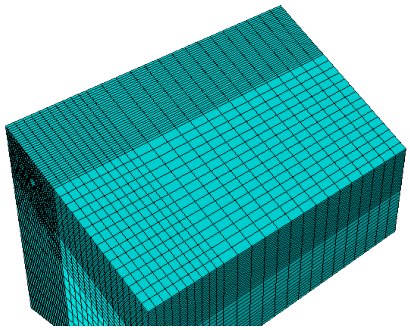

Figure 3: 3-D Model with typical mesh

2.3 Validation of FE Model

Before going into detailed analysis in this study, the FE model is validated using the experimental result available in Gu et al. (2022). During experimental work, the pipeline was subjected to an internal pressure of 10 MPa followed by a transverse displacement of 1 m. The stresses along the length of the pipeline were measured employing strain gauges after applying 1m displacement. Figure 4 shows the comparisons of stresses obtained by FE analysis with test results. The curve with triangle markers indicates the test results and the curve with circle markers indicates the result obtained from FE analysis. The figure shows a good correlation between the test result and the FE analysis. The rest of the studies are conducted using these validated FE models.

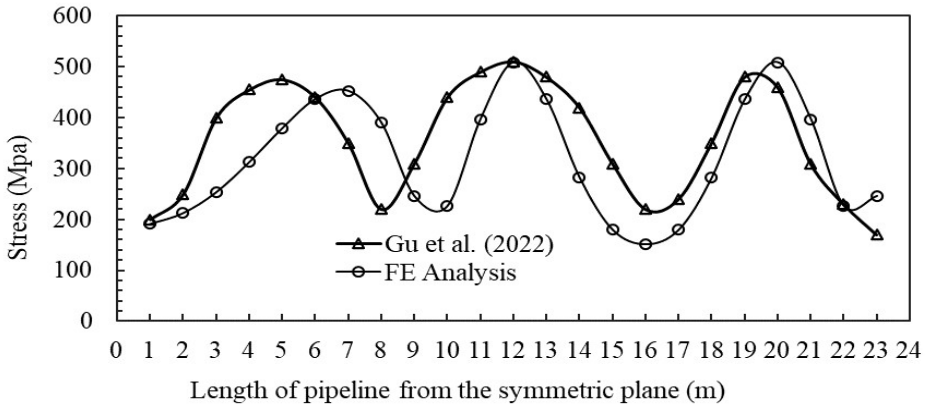

Figure 4: Validation of FE Model

2.4 FE Model of Corroded Pipe

During service life, the pipelines may be subjected to corrosion defects located on the exterior and/or interior surface of the pipeline. Mondal and Dhar (2017a) showed that both corrosion locations (i.e., exterior or interior) have almost similar effects on the performance of the corroded pipeline. Besides, the interaction between the pipeline and the soil body will be complicated in case of external corrosion defect. For these reasons, internal corrosion defect is considered for this study. The actual corrosion shape is irregular as shown in Figure 5 (a). Accepting the findings of other researchers, a rectangular shaped defect with a constant defect depth is used to simplify the corrosion defect model as shown in Figure 5 (b) (Mondal and Dhar 2017b, Gu et al. 2022, Netto et al. 2005 and Chen et al. 2015).

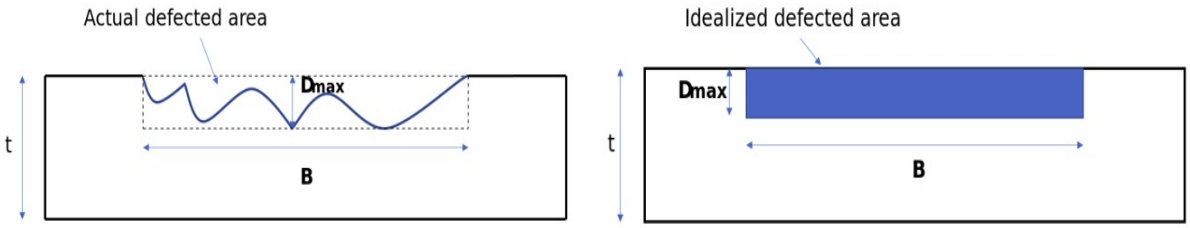

(a) Actual shape of corrosion defect (b) Idealised shape of corrosion defect

Figure 5: Shape of Corrosion Defect

Corrosion assessment methods are determined by normalising corrosion depth (d) and length (l) by the pipe wall thickness (t) (Arumugam 2019). The maximum allowable depth of carrion is 80% of wall thickness (ASME B31G 2015). The sizes of corrosion defect geometries considered in this investigation is given in Table 3. The FE models are analysed following two different stages. In the first stage, the pipelines are subjected to a constant displacement load and in the second stage, the deflected pipelines are subjected to varying internal pressure until failure. To investigate the effect of permanent ground displacement, three displacement magnitudes such as 0.5m, 1m and 1.5m are considered.

Table 3: Corrosion defect geometries

Pipe Size:	1016 mm (diameter), 22 mm (wall thickness)
Corrosion depth (d/t):	0.10, 0.20, 0.45, 0.60
Corrosion length (l/t):	5, 10, 15, 20

3. ANALYSIS AND DISCUSSION

3.1 Stress variation along the perimeter of the pipeline

From a preliminary analysis, it is observed that along with the displacement, the stress condition of the pipeline changes rapidly. Bending deformation of the pipeline is highest at the middle of the pipeline where the landslide thrust attacks, leading to stress variation along the cross-section along the cross section. The maximum stress is noticed to occur at the compressive side and at the tensile side. The compressive side is denoted by point A and the tensile side is denoted by point B shown in Figure 6. The tensile side goes under fracture when the tensile strain crosses the limiting strain. Therefore, the simulation focuses on the corrosion defect at point B due to its higher vulnerability and further simulation is done focusing on this point. The rest of the study on the corroded pipeline involves applying corrosion defects specifically at the tensile side.

3.2 Stress variation along the thickness and length of the pipe

By FE analysis, the von Mises stresses are calculated at four nodes along the remaining ligament of the corroded zone. The values of d/t and l/t of the pipe are 0.45 and 20 respectively. The nodes are defined as inner node, intermediate node 1, intermediate node 2 and outer node as shown in Figure 7. A complete analysis is done following three loading stages. In the first stage, the pipeline is subjected to gravity load followed by PGD of 1 m in the second stage. In the third stage, the pipeline is subjected to internal pressure.

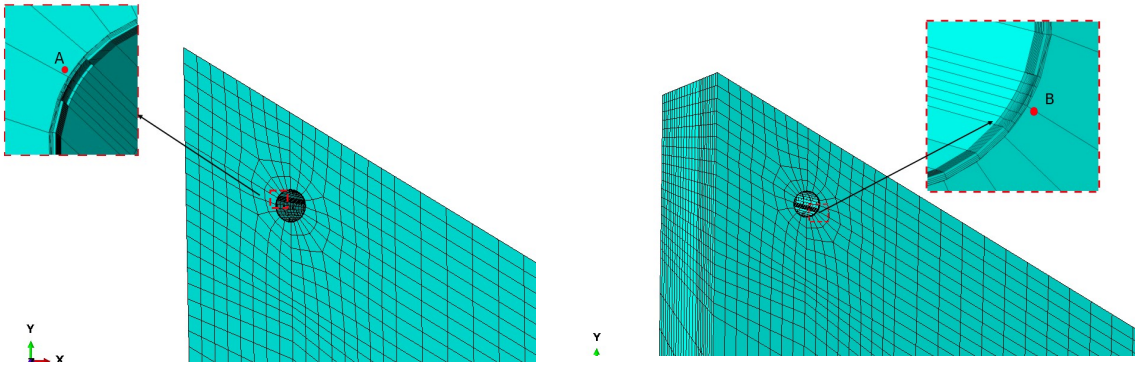

Figure 6: Compressive Side and Tensile Side of pipe cross-section

Figure 8 shows the variation of von Mises stress at four nodes with respect to PGD (Figure 8 (a)) and internal pressure (Figure 8 (b)). The PGD and internal pressure exerts outward bending at the corroded zone resulting in high von Mises stresses which indicates that the PGD reduces the remaining strength of the corroded pipeline.

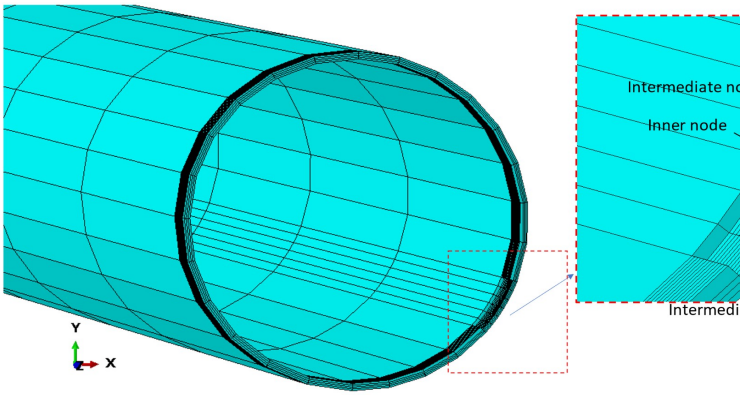

Figure 7: Node number along the thickness located the centre of the defected zone

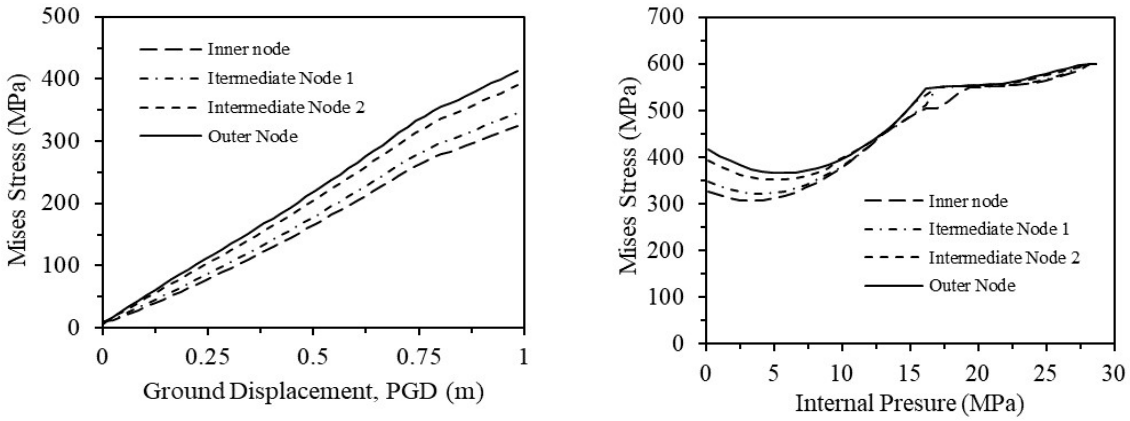

(a) Permanent Ground Displacement (b) Internal Pressure

Figure 8: Compressive Side and Tensile Side of pipe cross-section (with d/t=0.45, l/t=20)

Figure 9 shows the stress fluctuation along the axial length of the above-mentioned corroded pipe subjected to the said loadings. As depicted in the figure, the maximum von Mises stress appears at the corroded zone indicating the failure probability of the pipeline at the corroded zone.

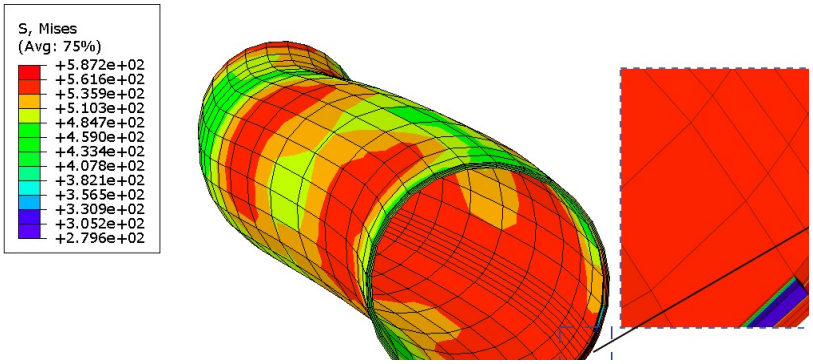

Figure 9: Stress variation along the length of the corroded pipeline (MPa)

3.3 Effect of PGD Magnitude

To investigate the effect of PGD magnitude on the performance of corroded pipelines, three FE models are developed using the corrosion geometries mentioned in section 3.2. The models are analysed for three PGD magnitudes of 0.50m, 1.0m and 1.5m. For each PGD magnitude, the average von Mises stresses through the corroded ligament located at the centre of the corrosion defect are calculated. The effect of PGD magnitudes is shown in Figure 10 in terms of Mises stress. The stresses are presented with respect to the time of analysis, where the models are subjected to gravity load, PGD and internal pressure from the time of 0-5, 5-10 and 10-15, respectively. The figure implies that the PGD magnitudes greatly influence the remaining strength of the corroded pipeline.

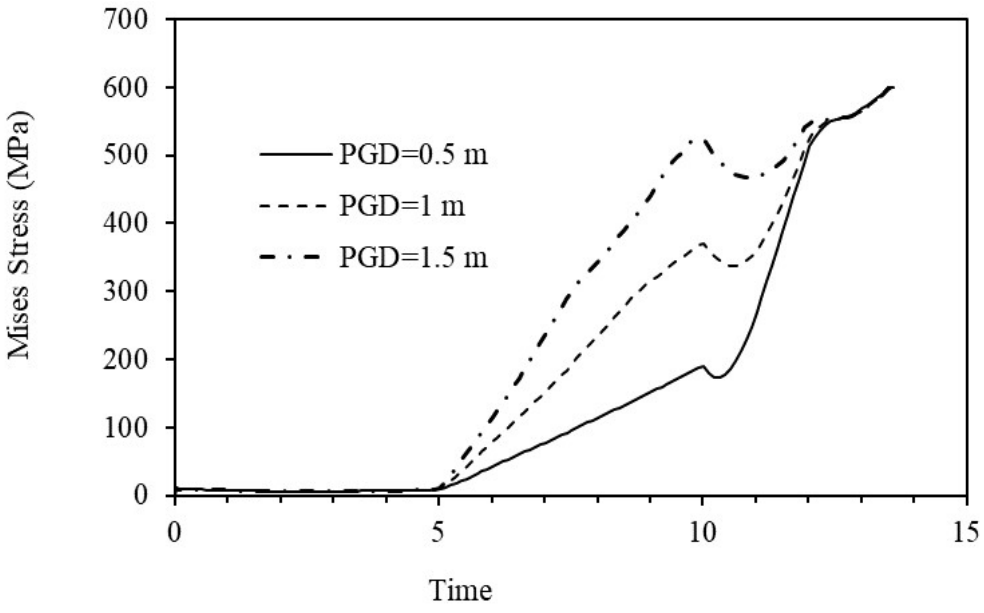

Figure 10: Effect of PGD magnitudes on the strength of pipeline

3.4 Effect of Corrosion Geometries

The corrosion geometries are defined in terms of corrosion depth (d) and corrosion length (l). To investigate the effect of d/t and l/t on the remaining strength of the corroded pipeline, nine FE models are developed using the corrosion geometries given in Table 3. The influence of corrosion depth is investigated with constant l/t of 20 and the influence of corrosion length is investigated with a constant d/t of 0.45. Figure 11 shows the effect of corrosion geometries in terms of Mises stress variation. The figure clearly implies that the remaining strength of corroded pipelines is significantly influenced by the corrosion geometries.

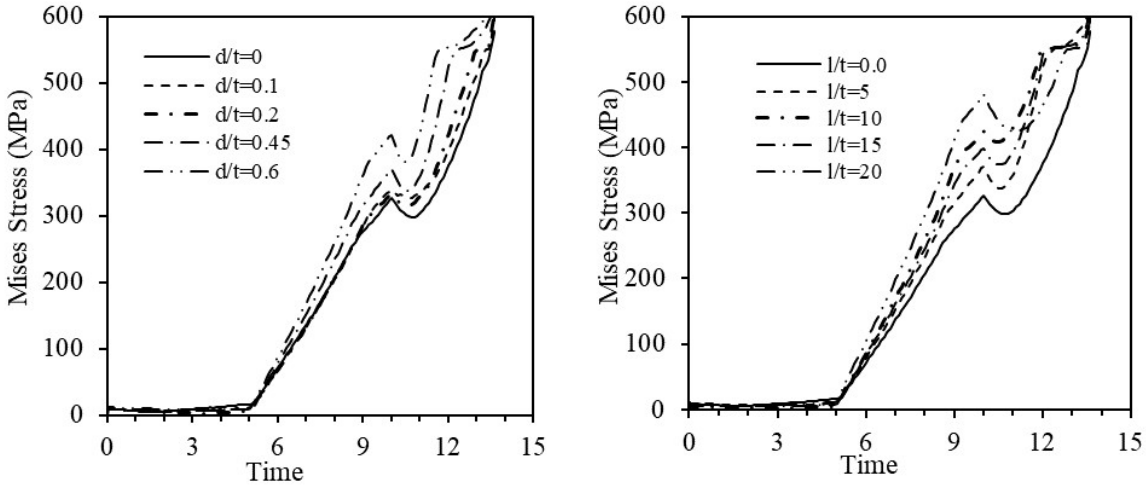

(a) Effect of d/t (with l/t=20) (b) Effect of l/t (with d/t=0.45)

Figure 11: Effect of corrosion geometries on the performance of corroded pipeline

4. DEVELOPMENT OF FAILURE ENVELOPE

4.1 Failure Criteria

To determine the remaining strength of a corroded pipeline in terms of burst pressure under a magnitude of PGD, it is essential to define the failure criteria at the beginning at the beginning. The existing literature shows that the burst pressure of a corroded pipeline is defined using the ultimate tensile strength of the pipe material. Applying this criterion in this study, the burst pressure of a corroded pipeline is determined when the average von Mises stress through the corroded ligament is equal to the ultimate strength of the corroded pipeline (i.e., 550 MPa). The burst of the intact pipeline (P_o) is determined using Eq. 1 available in Mondal and Dhar (2018), where t, D and σ_u indicate the pipe wall thickness, pipe nominal diameter and ultimate strength of the pipe material. From a preliminary analysis, it is observed that along with the displacement, the stress condition of the pipeline changes rapidly.

$$P_o = \frac{2t}{(D \quad 2t)}\sigma_u \qquad (1)$$

4.2 Failure Envelope

To ensure the uninterrupted operation of a pipeline network, the maximum operating pressure should be predicted accurately with proper precision. From the above discussions, it is observed that the remaining strength/burst pressure (P) of a pipeline depends on pipe dimensions, corrosion geometries, material properties and PGD magnitudes. Therefore, the burst pressure of a corroded pipeline should

be determined considering all of the influencing factors. In this study, some failure loci are constructed to predict the burst pressure of a corroded pipeline subjected to a PGD magnitude. In constructing the failure loci, the burst pressures (P) and the PGDs are normalised by the burst pressure of intact pipeline (P_o) and the pipe diameter (d), respectively. The corrosion geometries are represented by the corrosion area (a) which is the product of corrosion length (l) and corrosion depth (d) (i.e., a=l x d). The corrosion area (a) is normalised by pipe cross-sectional area (A). The pipe cross-sectional, A, is calculated using Eq.2, where D_o and D_i indicate the outer diameter and inner diameter of the pipe, respectively.

$$A = \frac{\pi}{4}\left(D_o^2 - D_i^2\right) \qquad (2)$$

Figure 12 shows the failure envelope constructed in this study for three PGD magnitudes. The figure can be a useful tool for oil and gas industries for assessing the remaining strength of corroded pipelines subjected to landslide and/or land subsidence related problems.

5. CONCLUSIONS

The study investigates the effect of PGD on the performance of corroded pipelines when subjected to internal pressure. The key findings can be summed up as follows:

- Under the action of PGD, maximum stress developed in the corroded zone of the pipe. The corrosion defect located at the tensile side of the pipeline is more harmful compared to the compressive side.
- The internal pressure in association with PGD causes higher local bending resulting in higher von Mises stress. The effect of corrosion geometries on the remaining strength of corroded pipelines is increased by the presence of PGD.
- Failure envelope between normalised failure pressure and the normalised corroded area is constructed for different PGD magnitudes. The envelope can be used for assessing the safe operating pressure of the corroded pipelines.

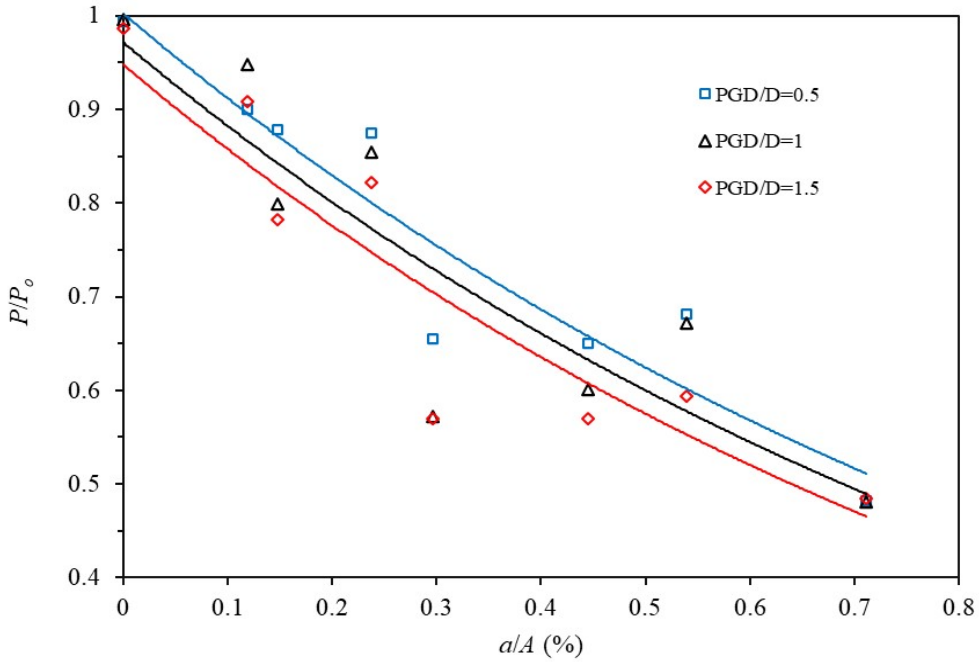

Figure 12: Failure Locus for Corroded Pipe Subjected Internal pressure with PGD

REFERENCES

Vazouras, P., Karamanos, S.A. and Dakoulas, P. (2010). Finite element analysis of buried steel pipelines under strike-slip fault displacements. *Soil Dynamics and Earthquake Engineering*, 30(11):1361-1376.

Lee, E.M., Fookes, P.G. and Hart, A.B. (2016). Landslide issues associated with oil and gas pipelines in mountainous terrain. *Quarterly Journal of Engineering Geology and Hydrogeology*, 49(2): 125-131.

Randolph, M.F., Seo, D. and White, D.J. (2010). Parametric Solutions for Slide Impact on Pipelines. J. Geotech. Geoenviron. Eng., 136(7):940-949.

Zhu, H. and Randolph, M.F. (2010). Large Deformation Finite-Element Analysis of Submarine Landslide Interaction with Embedded Pipelines. Int. J. of Geomech., 10(4): 145-152.

Liao, Y., Liu, C., T. Wang, T., Xu, T., Zhang, J. and Ge, L. (2021). Mechanical behavior analysis of gas pipeline with defects under lateral landslide. *Proc Inst Mech Eng C J Mech Eng Sci*, 235(23):6752-6766.

Agbo, S., Roy, K., Adeeb, S. and Li, Y. (2022). Effect of Permanent Ground Deformation Patterns on Strain Demand of Pressurized Buried Continuous Steel Pipelines. J. Pipeline Syst. Eng. Pract., 13(4):04022042.

Rajani, B.B., Robertson, P.K. and Morgenstern, N.R. (1995). Simplified design methods for pipelines subject to transverse and longitudinal soil movements. *Can. Geotech. J., 32*:309–323.

O'Rourke, M.J., Liu, X.J. and Flores-Berrones, R. (1995). Steel Pipe Wrinkling due to Longitudinal Permanent Ground Deformation. *J. Transp. Eng.*, *121*:443–451.

Benjamin, A.C., Freire, J.L.F. and Vieira, R.D. (2007). Part 6: Analysis of pipeline containing interacting corrosion defects. *Exp Tech*, 31(3):74-84.

Wang, Y., Zhang, P., Hou, X.Q. and Qin, G. (2020). Failure probability assessment and prediction of corroded pipeline under earthquake by introducing in-line inspection data. *Eng Fail Anal*, 115

Zhang, J., Liang, Z. and Han, C. (2016). Mechanical Behavior Analysis of the Buried Steel Pipeline Crossing Landslide Area. J. Press. Vessel Technol. 138:051702.

Zang, X., Gu, X., Wang, Q. and Cao, P. (2020). Study on finite element model of buried pipeline impacted by deep circular arc landslide. *Energy Chem. Ind., 41*: 65–70.

Cao, P., Gu, X., Zang, X., Lian, H., Mou, W. and Guo, Y.(2020). Effect of lateral landslide in frozen soil area on strain of the buried pipeline. *China Petro. Mach.*, *48*:141–146.

Gu, X., Zhang, Y., Huang, C., Luo, X., Zhang, H., Zhou, R. and Qiu, Y. (2022). Sensitivity Analysis of Influencing Factors of Gas Pipelines with Corrosion Defects under the Action of Landslides," in Energies (Basel), vol. 15, no. 18, Sep 2022.

Wang, X., Liu, Y., Hou, J., Li, S., Kang, Q., Sun, S., Ji, L., Sun, J. and Ma, R. (2020). The relationship between synsedimentary fault activity and reservoir quality—A case study of the Ek1 formation in the Wang Guantun area, China. *Interpretation*, *8*:SM15–SM24.

BS 7910. (2013). Guide to Methods for Assessing the Acceptability of Flows in Metallic Structure, British Standard Institution.

Mondal, B.C. and Dhar, A.S. (2017a). FE Evaluation of Burst Pressure Models for Corroded Pipelines. Journal of Pressure Vessels and Piping, ASME, 139(2): 1-8

Mondal, B.C. and Dhar, A.S. (2017b). Interaction of Multiple Corrosion Defects on Burst Pressure of Pipelines. Canadian Journal of Civil Engineering, 44(8): 589-597.

Netto, T. A., Ferraz, U. S. and Estefen, S. F. (2005). The effect of corrosion defects on the burst pressure of pipelines. *J Constr Steel Res*, 61(8):1185-1204.

Chen, Y., Zhang, H., Zhang, J., Liu, X., Li, X. and Zhou, J. (2015). Failure assessment of X80 pipeline with interacting corrosion defects. *Eng Fail Anal*, 47:67-76.

ASME, B31G. (2012). Manual for Determining the Remaining Strength of Corroded Pipelines. American Society of Mechanical Engineers, New York.

Mondal, B.C. and Dhar, A.S. (2018). Improved Folias Factor and Burst Pressure Models for Corroded Pipelines. Journal of Pressure Vessels and Piping, ASME, 140(1): 011702.